Journal of Cellular Automata, Vol. 8, pp. 383–393
Reprints available directly from the publisher
Photocopying permitted by license only

Cellular Model of Room Evacuation Based on Occupancy and Movement Prediction: Comparison with Experimental Study

PAVEL HRABÁK*, MAREK BUKÁČEK AND MILAN KRBÁLEK

Department of Mathematics, Faculty of Nuclear Sciences and Physical Engineering, Czech Technical University in Prague, Trojanova 13, 120 00 Prague 2, Czech Republic

Received: December 28, 2012. Accepted: May 31, 2013.

A simple experiment of non-panic evacuation of single room with one exit was organized and analyzed from the microscopic point of view. The rule-based CA based on Floor-Field model is presented to support the experiment. Several ideas of decision-making allowing the individual to choose an occupied cell are implemented to reflect observed behavior in the congestion cluster in front of the bottleneck. The velocity of pedestrians is represented by the updating frequency of individuals. Model parameters were calibrated to match the observations of the leaving-the-room experiment.

Keywords: Evacuation model, floor-field, occupation and movement prediction, egress experiment, shape of pedestrian cloud, time scale calibration.

1 INTRODUCTION

The model presented in this article is primarily designed to support the experimental study of pedestrian cloud formation in front of the exit during non-panic evacuation of single room without obstacles. Analogically to [1], the experiment is evaluated from the microscopic point of view.

An egress simulation model should reflect important features observed in the real system [2]. Several ways of describing pedestrian interaction by the so called social force appeared in [3], being suitable not only for evacuation

* E-mail: pavel.hrabak@fjfi.cvut.cz

purposes [4], but for other crowd features as well [5]. Such approach is very attractive but mostly not applicable for fast real-time simulations. In this case, the computational power of Cellular Automata should be used. For elaborate summary of CA application in pedestrian dynamics we refer the reader to [6] or [7].

The inspiration for the model presented in this article is the Floor-Field model [8, 9] and its implementation in F.A.S.T [5, 6, 10]. Similarly to this model, the potential field is considered, but unlike it, the desired line formation is reached using *bounds* rather than the dynamical field. This is closely related to the possibility of choosing an occupied cell [11]. To handle the problem of diagonal movement symmetrization (discussed e.g. in [10,12,13], or [14]) the probability- and time-penalization of diagonal movement is implemented. Inspired by [15, 16], and [17], simple movement prediction is taken into account. Furthermore, essential change in the potential iso-curves solves elegantly the problem of wall repulsion mentioned in [18].

2 EXPERIMENT - OBSERVATION

This article is based on the leaving-the-room experiment organized with help of 86 volunteer students of the Faculty of Nuclear Sciences and Physical Engineering. The experiment was held in the study room in Trojanova building (Trojanova 13, Prague 2). The purpose of the experiment was to investigate the shape of pedestrian cloud and cluster formation in front of the single door of 7 m wide and 13 m long room schematically depicted in Figure 3. According to specific setting (see Figure 1), 28 or 30 participants were arranged in the room. After initiation, everyone started to move towards the door. Participants were only briefly instructed to follow three basic rules: leave the room as fast as possible; do not run, just walk; avoid physical contact.

These restrictions protected the participants from injuries, they were not motivated to furious evacuation. This procedure was repeated 23 times and recorded by a camera placed above the exit door; snapshots of the recording are shown in Figure 2. An additional detector was placed at the door, which recorded the evacuation time of each pedestrian.

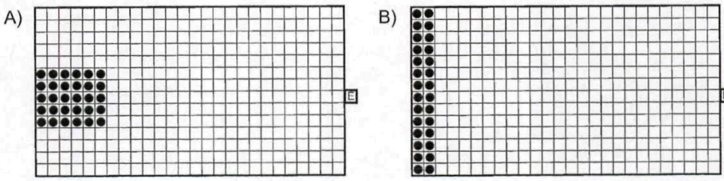

FIGURE 1
Initial setting of the experiment. Black circles represent pedestrians, cell E represents the exit.

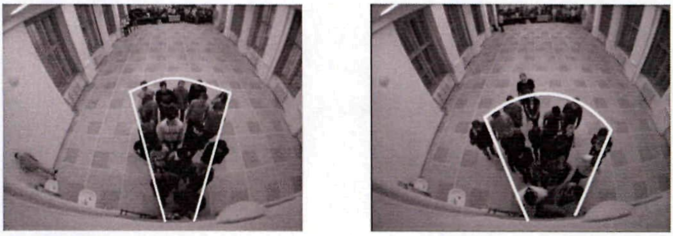

FIGURE 2
Snapshots from the cluster-forming at the door approximately 9 seconds after initiation. Funnel like shape of the cluster was observed.

Considering the essence of the experiment, participants were not highly motivated to leave the room earlier than others. Therefore, there has not been observed any drastic fight at the door. This avoided the participants to create the semi-spherical cluster in front of the exit, which is expected in panic-like situations (see e.g. [4, 7]). A multi-line (chaotic) queue is formed instead, which leads to the funnel-like formation. Furthermore, pedestrians hold the initial formation and wait rather than walking around the crowd. These effects were observed for any initial formation.

3 RELATED MODEL

This chapter introduces simple model containing new ideas of individual motion improvement on the microscopic level. The goal was to capture and mimic the non-panic behavior observed during the experiment.

3.1 Floor-Field Bases of the Model

For purpose of the simulation the room was divided in square-shaped cells with the lattice constant corresponding to 0.5 m. Every cell is identified by the position vector $\vec{x} = (x_c, x_r)$ of the cell center, where the exit cell $\vec{e}$ is placed to the origin, $\vec{e} = (0, 0)$, as depicted in Figure 3. The indices c and r

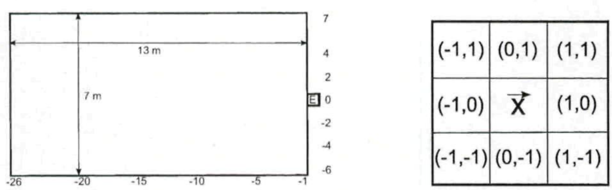

FIGURE 3
Left: Experiment was performed in a rectangle room 7 m wide and 13 m long. Right: Moore's neighborhood with range 1 of cell $\vec{x}$ with indexation used in this article.

stand for column and row respectively. The static field $U(\vec{x})$ represents the potential generated by the exit $\vec{e}$ and is calculated by

$$U(\vec{x}) = F \cdot \varrho(\vec{e}, \vec{x}) \ , \quad \text{where} \quad \varrho(\vec{e}, \vec{x}) = \left(|e_{\mathrm{c}} - x_{\mathrm{c}}|^2 + |e_{\mathrm{r}} - x_{\mathrm{r}}|^2\right)^{\frac{1}{2}} \tag{1}$$

is the Euclidian distance of the cell $\vec{x}$ to the exit $\vec{e}$, and $F \in (0, +\infty)$ is the strength parameter of the potential determining the attraction strength of the exit $\vec{e}$ (high value of F suppresses stochastic character of the motion). Another static property of the cell is expressed by the *cell type number* $t(\vec{x})$, which determines, whether the individual can enter the cell ($t(\vec{x}) = 1$), e.g. floor cell, exit; or not ($t(\vec{x}) = 0$), e.g. wall, barrier.

The dynamical status of every cell is determined by the *occupation number* $n(\vec{x})$ identifying whether the cell is empty ($n(\vec{x}) = 0$) or occupied by one individual ($n(\vec{x}) = 1$), and the *prediction number* $r(\vec{x}) \in \{0, 1, \ldots\}$, which denotes the number of individuals being predicted to enter the cell $\vec{x}$. The individual is predicted to continue in the same direction as it moved in his previous step. The exit cell $\vec{e}$ is understood being always empty, keeping the rule that only one individual can enter the cell during one time step.

The essence of the CA dynamics lies in rules, according to which the individual chooses next target cell. In presented model, the individual decides stochastically. The probability $p_{\vec{d}}(\vec{x})$ of choosing the cell $\vec{x} + \vec{d}$ from the target neighborhood $S_T(\vec{x})$ depends on the current state of the reaction neighborhood $S_R(\vec{x})$, i.e

$$p_{\vec{d}}(\vec{x}) = \Pr\left\{\vec{x} + \vec{d} \;\middle|\; S_R(\vec{x})\right\} \ . \tag{2}$$

The probability $p_{\vec{d}}(\vec{x})$ chosen for purposes of this article is a compilation of approaches presented in [8,9], and [17]. The concept of potential field is adopted from [8], the occupation and movement prediction are taken from [9] and [17]. In this article, the neighborhood according to Moore's definition with range 1 is chosen for both, the target and the reaction neighborhood, i.e. $S_T(\vec{x}) = S_R(\vec{x}) = \vec{x} + S_M$, where

$$S_M = \{(-1, 1); (0, 1); (1, 1); (-1, 0); (1, 0); (-1, -1); (0, -1); (1, -1)\} \tag{3}$$

(see Figure 3). Here, $\vec{d} \in S_M$ is referred to as *direction*. The definition (3) implies that the individual cannot choose his current position $\vec{x}$ during the decision process (it does not mean that he *has* to move; see subsection 3.2).

Let us now denote $\vec{d}_r(i)$ the currently predicted direction of the individual i. The movement prediction from the view of the individual i is then

$$r_i'(\vec{d}) = r(\vec{x} + \vec{d}) - \delta_{\vec{d},\vec{d}_r(i)} \ , \tag{4}$$

where for $a, b \in S_M$ we define $\delta_{\vec{a},\vec{b}} = 0$ if $\vec{a} \neq \vec{b}$ and $\delta_{\vec{a}\vec{a}} = 1$. For all $\vec{d} \in S_M$ the indicator $\widetilde{r}_i(\vec{d}) = 1 - \delta_{0,r_i'(\vec{d})}$ indicates, whether the cell $\vec{x} + \vec{d}$ is predicted to be entered by another individual than i or not.

The notation presented above allows us to extend the simple potential-field-based decision process by the occupation and movement prediction, which is crucial for the principle of *bounds* presented below. The probability that the individual i sitting in the cell $\vec{x}$ chooses the direction $\vec{d}$ is given by

$$\begin{aligned} p_{\vec{d}}(\vec{x}) = \mathcal{N} \cdot C(\vec{d}) \cdot t(\vec{x} + \vec{d}) \cdot \exp\{-\alpha \cdot U(\vec{x} + \vec{d})\} \times \\ \times [1 - \beta \cdot n(\vec{x} + \vec{d})] \cdot [1 - \gamma \cdot \widetilde{r}_i(\vec{d})] \ , \end{aligned} \tag{5}$$

where $\mathcal{N}$ is the normalization constant ensuring that $\sum_{\vec{d} \in S_M} p_{\vec{d}}(x) = 1$, and coefficients $\alpha, \beta, \gamma \in \langle 0, 1 \rangle$ are coefficients of sensitivity to the potential, occupation number, and prediction number respectively. The sensitivity parameters determine the influence of the potential, occupation, or prediction on the individual's choice of the target cell. These parameters are to be determined later and their influence is demonstrated in Figure 4.

To eliminate differences in motion in different angles caused by the rectangular nature of the lattice, the diagonal movement penalization $C(\vec{d})$ was added to (5). $C(\vec{d}) = c \in (0, 1)$ for diagonal movement ($d_c \cdot d_r \neq 0$) and

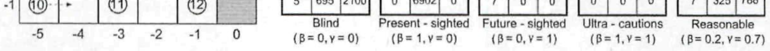

FIGURE 4
Example illustrating principle of decision of an individual in the cell $\vec{x}$ as visualized in subfigure A. Dashed arrows represent predicted movement of neighboring individuals. The probability distribution $p_{\vec{d}}(\vec{x})$ given by (5) is determined by potential, occupation and prediction number. Subfigure B visualizes these parameters. Darker color represents lower potential (closer to exit), hatched area means penalization in stated category. Final probabilities for different settings of sensitivity parameters β, γ are shown in subfigure C. For each of them, 10 000 decisions were divided into cells according to (5) with $F = 3, \alpha = 1$.

$C(\vec{d}) = 1$ otherwise. The constant c was determined by means of the symmetry analysis of the evacuation time and was set to $c = 0.2$.

3.2 Individual Movement and Inovations

The goal of this subsection is to explain the interaction of all individuals within considered time period as a whole. Innovative concept of varying individual's updating frequency and principle of *bounds* are introduced. One update of the system can be divided in four phases:

1. *Selection of active individuals* means that only individuals that are supposed to move at considered time are activated. Each individual i has his *own updating frequency* of motion f_i which determines individual's *own updating period* $T_i = f_i^{-1}$. This quantity corresponds to the time lag until individual's next activation. In principle, whenever the individual moves, or tries to move, at time t, the time of his next activation is set to $t + T_i$. The only situation, when this rule changes, is after the diagonal movement. Because the diagonal movent is $\sqrt{2}$-times longer, it takes $\sqrt{2}$-times more time. This leads to the diagonal movement time-penalization (similar approach to handle the diagonal movement symmetrization has been applied in [13]), and the next activation time is set to $t + qT_i$, where q is the rational approximation of $\sqrt{2}$, e.g $q = 3/2$. The rational approximation of $\sqrt{2}$ is necessary to keep sufficiently discrete structure of time for long period. Using this approach we can consider heterogenous system of individuals with varying desired velocity (frequency) keeping the nearest-neighbor interaction. Here we make a remark that the time penalization of diagonal movement relies to the time span only and does not influence the probability $p(\vec{d})$. Therefore, the time and the probability penalization are independent features in the model.
2. *Decision process* of all individuals proceeds simultaneously and consists in choosing the direction according to given rules explained in section 3.1. If the target cell is empty, the individual is added to the *waiting list* of the cell. If the target cell of individual i is occupied by another individual j, the *bound* of i to j is created. Individual j is called the *blocker* and individual i becomes *bounded*. The bound holds until next update of the bounded individual i or until the motion of the blocker j.
3. *Conflict solution and motion*. It is obvious that the two-dimensional structure of the lattice connected to the independent decisions of individuals leads to variety of conflicts solved as follows:
   (a) More individuals choose the same unoccupied cell (the waiting list of the cell contains more then one individual). In this case the

movement of all individuals is disabled with probability μ playing role of the *friction parameter* (taken from [5]). Otherwise, i.e. with probability $(1 - \mu)$, one of the waiting individuals is chosen randomly to enter the cell, the others don't move.

(b) The individual chooses an occupied cell. In this case, the individual i predicts the movement of the blocker j and wants to take his place. If the blocker j moves (i.e. j is the single individual to enter the target cell or wins the conflict described in a)), the bounded individual i tries to enter his target cell. Again, if he is the only bounded individual to j, there is no conflict. If more then one individual are bounded to j, the occurring conflict is solved analogically to the conflict a). This rule is applied recursively to all bounded individuals.

4. *Time actualization*. New activation times of individuals are calculated. The global timer "jumps" to the closest event given by the nearest activation time of the individuals.

Here we note that during the conflict solution of type b) even a non-active individual can move in case, it is bounded to the blocker. This is illustrated by the example in Figure 5. The principle of conflict solution and bounds during one update is illustrated in Figure 6.

4 EXPERIMENT - MODEL CALIBRATION

Before the model comparison with the experiment, the values of potential strength F and diagonal penalization c have been determined. The choice

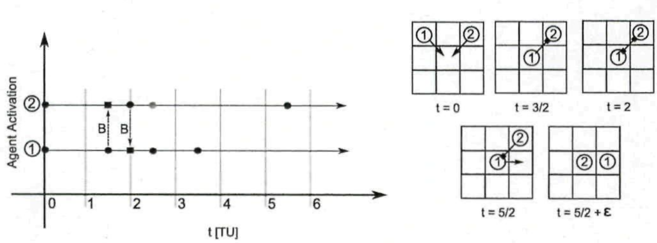

FIGURE 5
Example illustrating principle of bounds. Two individuals 1 and 2 with own periods $T_1 = 1$, $T_2 = 2$ are activated in time t=0 and decide to enter the same cell $(0, 0)$, individual 1 wins. Next update-time of individual 1 is set to $t = 3/2$ because of the diagonal movement, the individual 2 waits until $t = 2$. At $t = 3/2$ individual 1 decides to enter the cell (1,1) occupied by individual 2 and gets bounded to 2. At $t = 2$ individual 2 decides to enter (0,0) and gets bounded to individual 1. At $t = 5/2$ individual 1 cancels his bound and moves to (1,0). Due to the bound, individual 2 moves to (0,0) and his next-update time is set to $t = 5/2 + 2(3/2)$. The multiplication by $3/2$ is due to diagonal movement penalization.

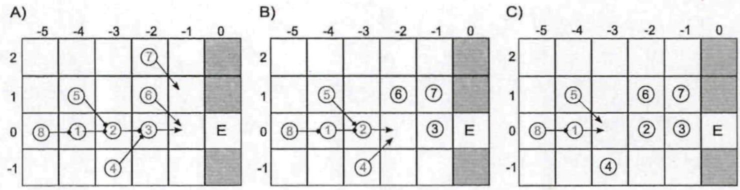

FIGURE 6
Example illustrating principle of waiting lists and bounds during one update. Every individual chooses the target cell and is either added in waiting list (triangles) or bounded to the blocker (squares) as shown in subfigure A. In this case, individual 7 is in the waiting list of cell (-1,1), individuals 3 and 6 in the waiting list of cell (-1,0), individual 4 and 2 are bounded to individual 3 etc. After conflict solution in waiting lists (subfigure B) the bounds induce conflict in cell (-2,0), which is solved analogically (subfigure C). Conflict in the cell (-3,0) will be solved in the same way and may finaly lead to the motion of individual 8.

$F = 3$ and $c = 0.2$ used for simulations balances the deterministic motion of an individual in free space with the stochastic behavior in the congested cluster independently on the position of source of the potential field (the exit in this case). This satisfies the symmetry requirements.

4.1 Funnel-Like Shape

At first instance we have tried to replicate the funnel-like shape of the pedestrian cluster at the exit by means of the microscopic movement of individuals by introducing the bounds. Observing the simulation we have discovered that the funnel shape is held only for a short time after the cluster formation. This motivate us to deform the spherical form of potential iso-value curves. For further simulation the following definition of potential was used:

$$\varrho(\vec{e},\vec{x}) = \sqrt{10(e_r - x_r)^2/(e_c - x_c) + (e_c - x_c)^2}\ . \tag{6}$$

These potential iso-value curves are presented in Figure 7. Here we note that Equation (6) is applicable to define the required potential modification

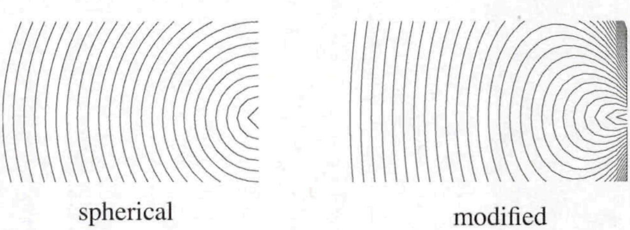

FIGURE 7
Demonstration of suggested potential.

only for normal conditions without obstacles, where the average direction of pedestrian cloud center towards the exit is in the positive x_c direction. The generalization for more complex geometries requires more detailed experimental study and further discussion.

4.2 Time-Span

To calibrate the time span of the model, i.e to give the relation of time units in the model (TU) and seconds in the experiment, we have compared the evacuation time from two different points of view. Firstly, the approximate velocity in free flow regime was measured by means of the time interval between the initiation and the egress of the first pedestrian or individual. Secondly, the average headway evolution of two successive pedestrians or individuals walking through the door has been compared.

Several sets of parameters were analyzed and the evacuation times compared. The goal was to match the free-flow time span to the condensed flow time span. This relation is fulfilled for $\beta = 0.2$, $\gamma = 0.7$, $\mu = 0.9$, i.e. the occupation number has significantly weaker impact than the prediction of other pedestrians movement. The high value of the friction parameter μ is closely related to the principle of bounds and different updating frequencies of the individuals. From the macroscopic point of view, the ratio of unresolved conflicts is lower than 40 %. During the simulation, homogenous group of individuals with own frequency $f = 1$ TU was considered. Under these conditions, the corresponding time span is 1 TU = 0.32 s.

To compare the time headway evolution the averaged time-headway of the n-th egressing pedestrian or individual was used. We have observed slightly increasing trend from 600 to 800 ms. Such behavior is observed in the calibrated model as well, see Figure 8.

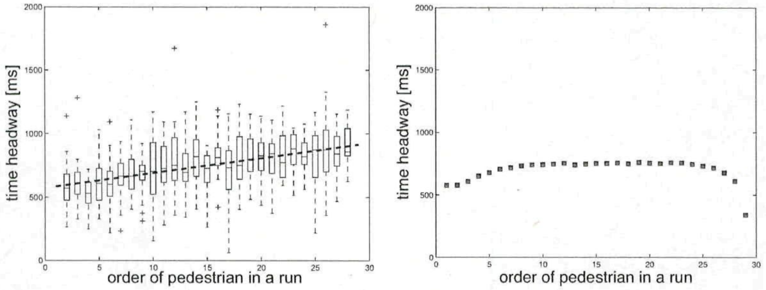

FIGURE 8

The time headway comparison. Left figure shows the boxplot of the time headway of pedestrians plotted against their order at the door. The right figure shows analogical values for the individuals in the simulation. The slight decrease for last 5 individuals is caused by the lack of conflicts at the door.

5 CONCLUSIONS

In this article several ideas of individual movent rules in Floor-Field based model were introduced that should better reflect the microscopic behavior of individuals during the egress simulation. Those ideas are supported by the experimental study performed with help of the group of students of the Faculty of Nuclear Sciences and Physical Engineering. Although the sample of pedestrians was quite homogenous, the model enables the simulation of heterogenous system by changing the own frequency, sensitivity to potential, prediction, or occupation.

In the model, the final cell attractiveness strongly depends on coefficients of sensitivity to stated parameters. Whereas the potential represents static conditions, occupation and prediction of conflict reflect the individual strategy. The ratio of sensitivity to prediction and the sensitivity to occupation is related to the aggression or herding characteristics.

We introduce the principle of bounds that leads to spontaneous line formation in the cluster. To balance the fast motion in lines with the observed delay at the doors, the friction parameter μ needs to be calibrated. The high value of μ is caused by the asynchronous time updates induced by the diagonal movement time penalization.

The resulting parameters matching to the performed experiment are as follows: the sensitivity to potential $\alpha = 1$, the potential strength $F = 3$, the sensitivity to occupation $\beta = 0.2$, the sensitivity to prediction $\gamma = 0.7$, the friction parameter $\mu = 0.9$. The time span with own frequency of individuals $f = 1$ TU is 1 TU = 0.32 s.

Considering the model applicability in real time simulations, presented modifications of the simple Floor Field model do not significantly slow down the simulation process. We have investigated the ratio between time consumed by the computer simulation and the evacuation time corresponding to the same simulation. Resulting mean value of the ratio for non-parallelized algorithm is 8.5×10^{-4} with maximum value of 2.6×10^{-3}. More detailed study would, of course, require the implementation of the algorithm in more complex geometries and situations.

In the future, we plan to investigate in detail the influence of stated parameters on the microscopic movement and conflict solution. This analysis helps us to improve the microscopic quantities as time headway between successive individuals at the door. We feel the challenge to generalize the model in more complex geometries and support the study by means of experiments.

ACKNOWLEDGEMENTS

This work was supported by the grant SGS12/197/OHK4/3T/14 and the research program MSM 6840770039. We would like to thank to GAMS members, especially Juraj Panek, for significant help with the experiment preparation and data processing.

REFERENCES

[1] Seyfried A., Portz A., Schadschneider A. (2010). Phase coexistence in congested states of pedestrian dynamics. In: *ACRI 2010, LNCS*, **6350**, 496–505.

[2] Klüpfel H., Schreckenberg M., Meyer-König T. (2005). Models for Crowd Movement and Egress Simulation. In: *Traffic and Granular Flow 03*, 357–372.

[3] Helbing D., Molnar P. (1995). Social force model for pedestrian dynamics. *Phys. Rev. E*, **51/5**, 4282–4286.

[4] Helbing D., Farkas I., Vicsek T. (2000). Simulating dynamical features of escape panic. *Nature*, **407**, 487–490.

[5] Schadschneider A., Seyfried A. (2009). Empirical results for pedestrian dynamics and their implication for cellular automata models. In: *Pedestrian Behavior: models, data collection and applications*, Bingley: Emerald Group Publishing .

[6] Kretz T. (2007). Pedestrian Traffic, Simulation and Experiments. PhD. thesis, Universität Duisburg-Essen, Germany.

[7] Schadschneider A., Chowdhury D., Nishinari K. (2010). *Stochastic transport in complex systems*. Amsterdam: Elsevier Science.

[8] Kirchner A., Schadschneider A. (2002). Simulation of evacuation processes using a bionics-inspired cellular automaton model for pedestrian dynamics. *Physica A*, **312**, 260–276.

[9] Nishinari K., Kirchner A., Namazi A., Schadschneider A. (2004). Extended floor field CA model for evacuation dynamics. In: *IEICE Trans. on Inf. and Syst.*, **E87-D**, 726–732.

[10] Kretz T., Schreckenberg M. (2006). The F.A.S.T. – model. In: *ACRI 2006, LNCS*, **4173**, 712–715.

[11] Henein C. M., White T. (2007). Macroscopic effects of microscopic forces between agents in crowd models. *Physica A*, **373**, 694–712.

[12] Klüpfel H. (2003). A Cellular Automaton Model for Crowd Movement and Egress Simulation. PhD. thesis, Universität Duisburg-Essen, Germany.

[13] Schultz M., Lehmann S., Fricke, H. (2007). A discrete microscopic model for pedestrian dynamics to manage emergency situations in airport terminals. In: *Pedestrian and Evacuation Dynamics 2005*, 369–375.

[14] Yamamoto K., Kokubo S., Nishinari K. (2007). Simulation for pedestrian dynamics by real-coded cellular automata (RCA). *Physica A*, **379**, 654–660

[15] Kretz T., Kaufman M., Schreckenberg M. (2008). Counterflow Extension for the F.A.S.T.-Model. In: Cellular Automata. LNCS, **5191**, 555–558.

[16] Steffen B. (2010). A Modification of the Social Force Model by Foresight. In: *Pedestrian and Evacuation Dynamics 2008*, 677–682.

[17] Sumaa Y., Yanagisawab D., Nishinari K. (2012). Anticipation effect in pedestrian dynamics: Modeling and experiments. *Physica A*, **391**, 248–263.

[18] Georgoudas I. G., Koltsidas G., Sirakoulis G. Ch., Andreadis I. Th. (2010). A Cellular Automaton Model for Crowd Evacuation and its Auto-Defined Obstacle Avoidance Attribute. In: *ACRI 2010, LNCS*, **6350**, 455–464.